Supporting Information

High Strength, Self-Healing Sensitive Ionogel Sensor Based on MXene/Ionic Liquid Synergistic Conductive Network for Human-Motion Detection

Xiao Wen[a]†, Zhipeng Deng [a]†, Hui Wang[b], Jianyang Shi[a], Shuang Wang[a], Haibo Wang[a,c]*, Yueming Song[a], Zongliang Du[a], Jinghong Qiu[a], Xu Cheng[a]*

[a] College of Biomass Science and Engineering; Orthopedic Research Institute, Department of Orthopedics, West China Hospital, Sichuan University, Chengdu 610065, China.

[b] West China School of Basic Medical Sciences and Forensic Medicine, Sichuan University, Chengdu 610041, PR China

[c] State Key Laboratory of Biobased Material and Green Papermaking, Qilu University of Technology, Shandong Academy of Sciences, Jinan 250353, China

† These authors contributed equally to this work.

*Corresponding authors: E-mail addresses: whb6985@scu.edu.cn (Haibo Wang), scuchx@163.com (Xu Cheng)

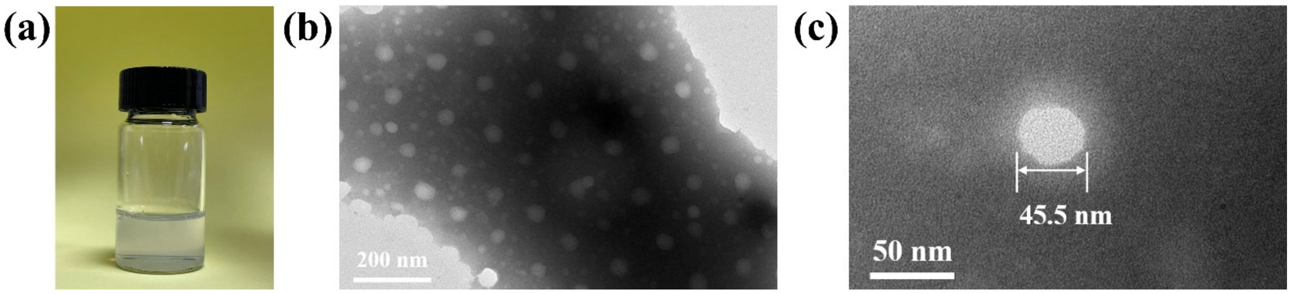

Fig. S1 (a) Waterborne polyurethane emulsion (WPU) image, (b) TEM image of WPU emulsion (c)TEM image of a typical emulsion particle.

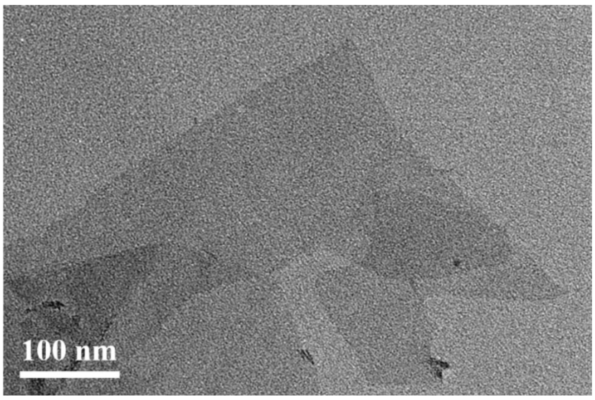

Fig. S2 SEM image of monolayer MXene

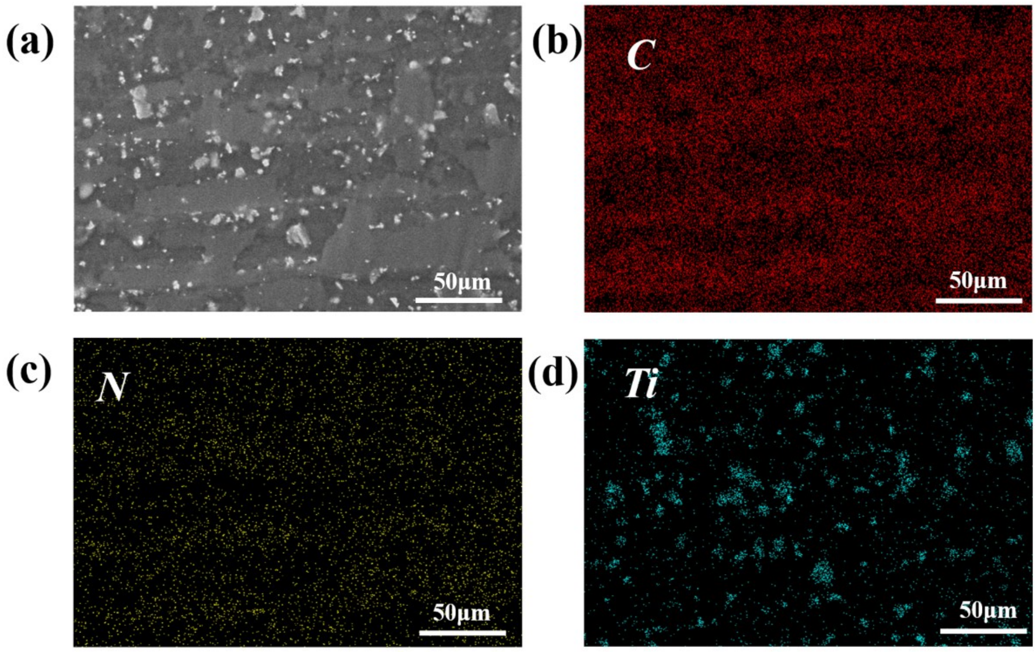

Fig. S3 (a) SEM images of MPI films and corresponding elemental mapping images of (b) Carbon, (c) Nitrogen and (d) Titanium.

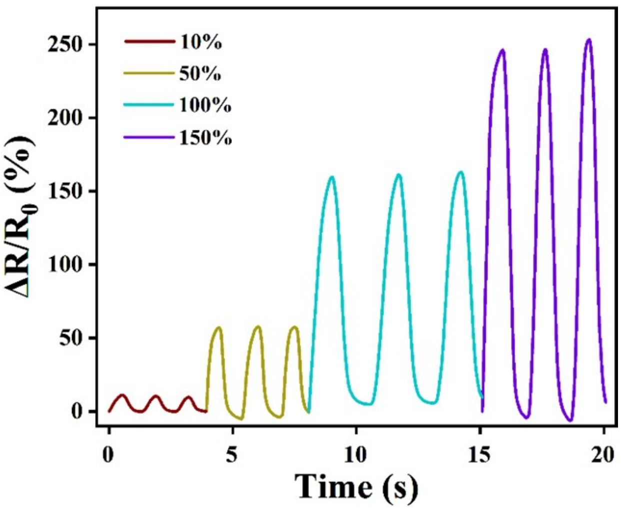

Fig. S4 The relative change of resistance ($\Delta R/R_0$) signals of MPI-2 at different strains.

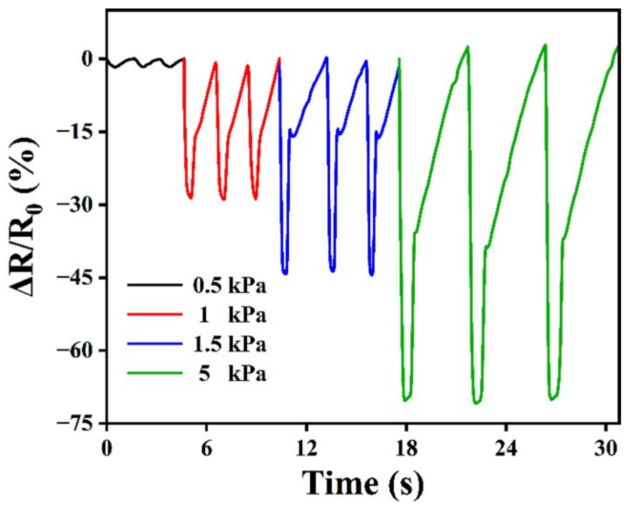

Fig. S5 The $\Delta R/R_0$ signals of MPI-2 at different pressures.

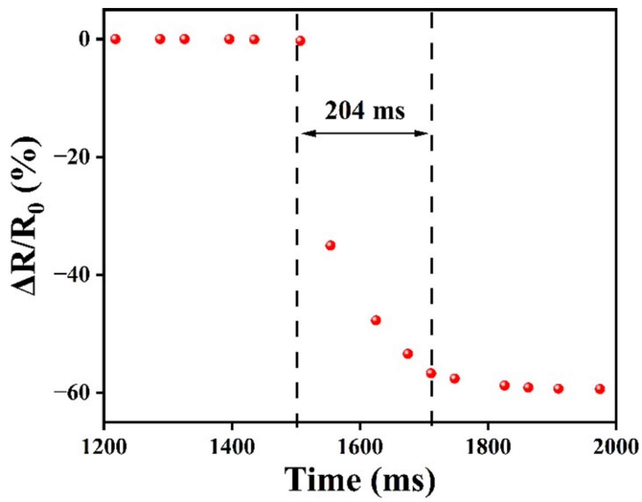

Fig. S6 The pressure response time of MPI-2.

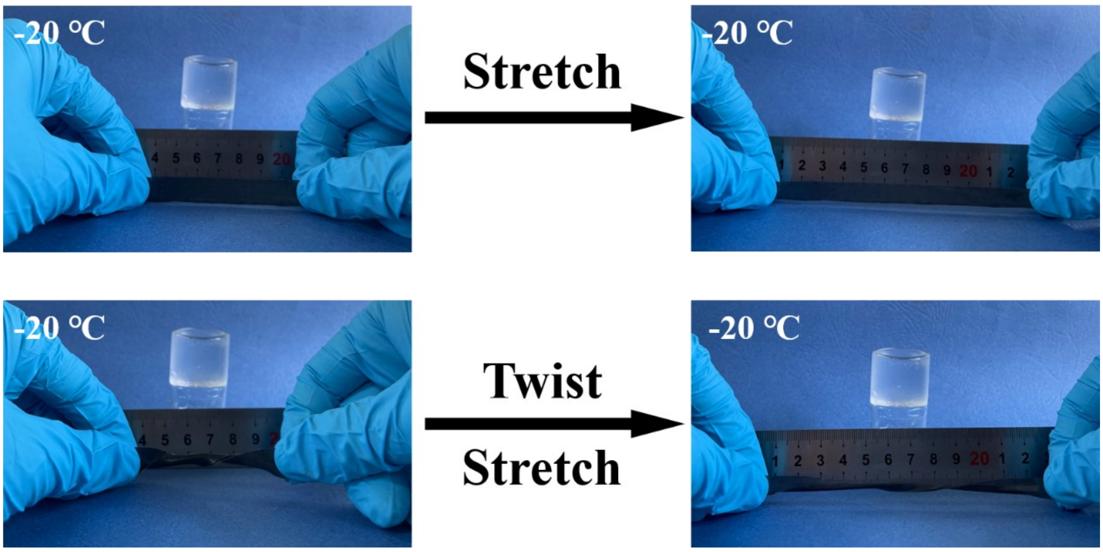

Fig. S7 The images of MPI-2 stretched and stretched after twisting at -20 °C.

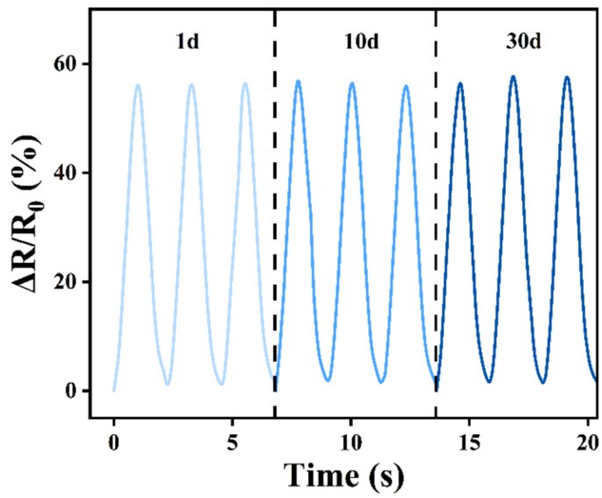

Fig. S8 The $\Delta R/R_0$ signals of MPI-2 after 10 and 30 days of storage at -20°C.

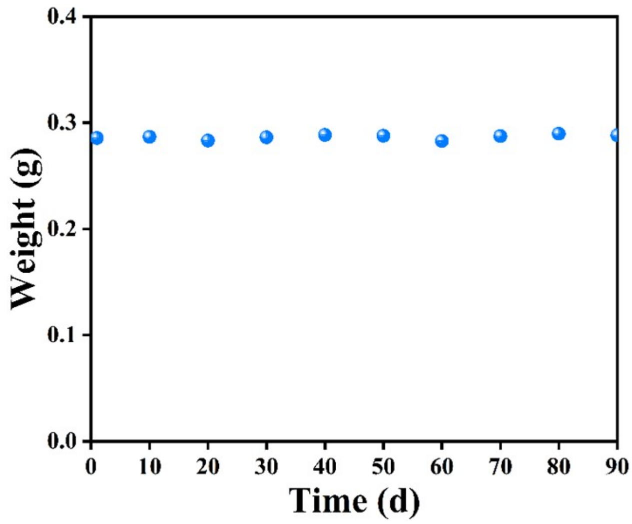

Fig. S9 Weight change of MPI-2 stored in open environment at room temperature for 90 days.

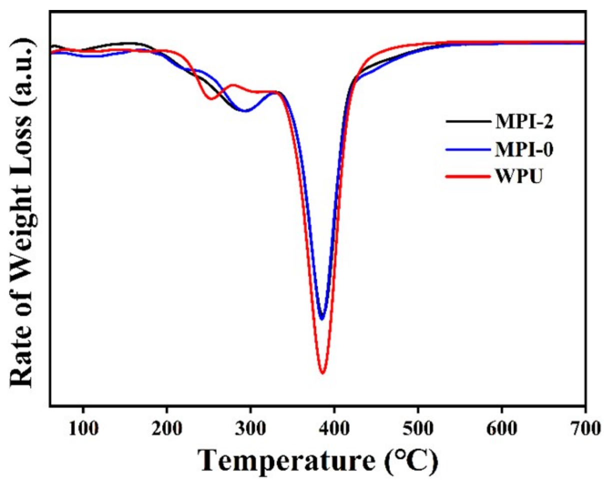

Fig. S10 The first order derivatives of the weight loss thermogram of MPI-2, MPI-0 and WPU.

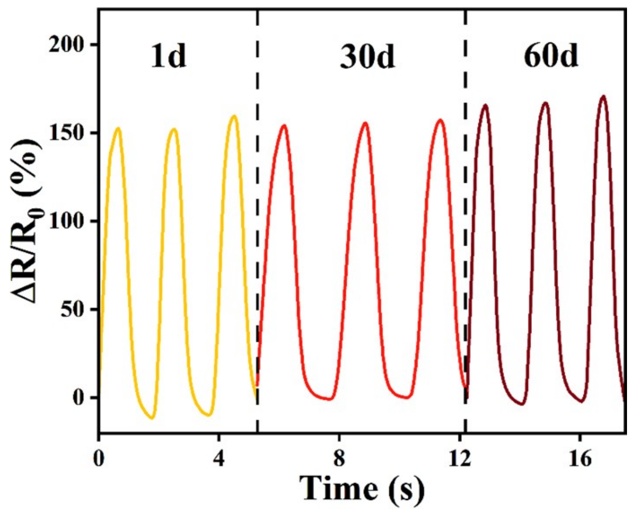

Fig. S11 The $\Delta R/R_0$ signals of MPI-2 stored in an open environment for 30 days and 60 days.

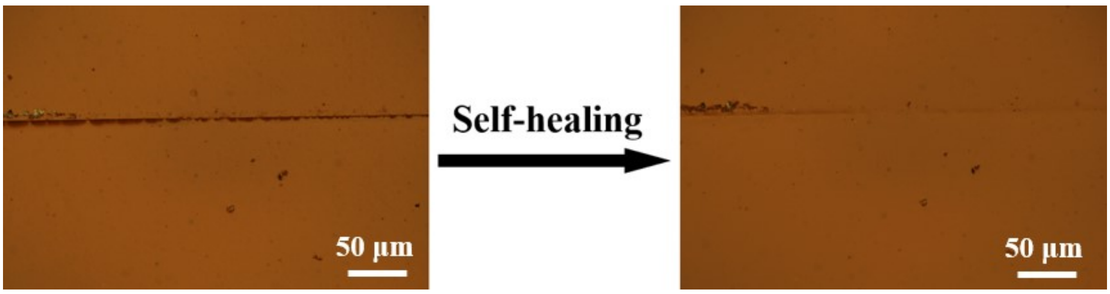

Fig. S12 The optical microscope photographs of MPI-2 after scratching and self-healing.

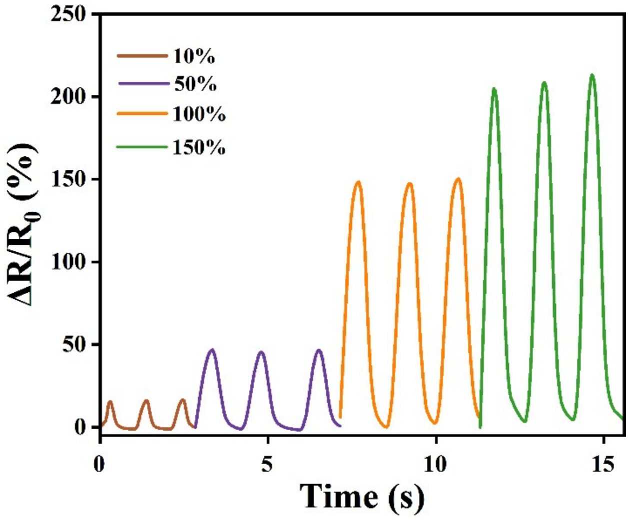

Fig. S13 The $\Delta R/R_0$ signals of MPI-2 at different strains after self-healing.

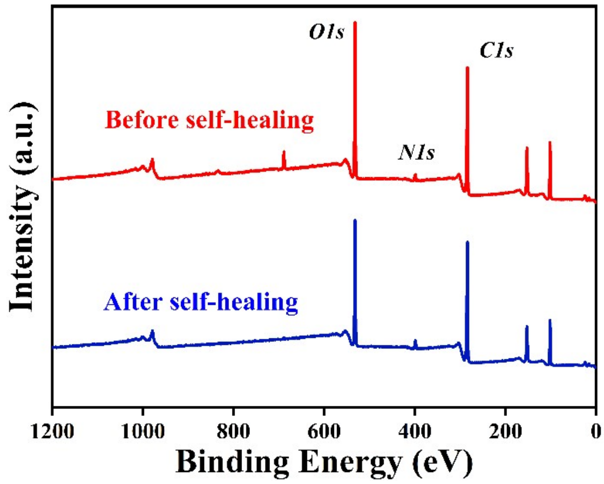

Fig. S14 The XPS images of MPI-2 before and after self-healing.

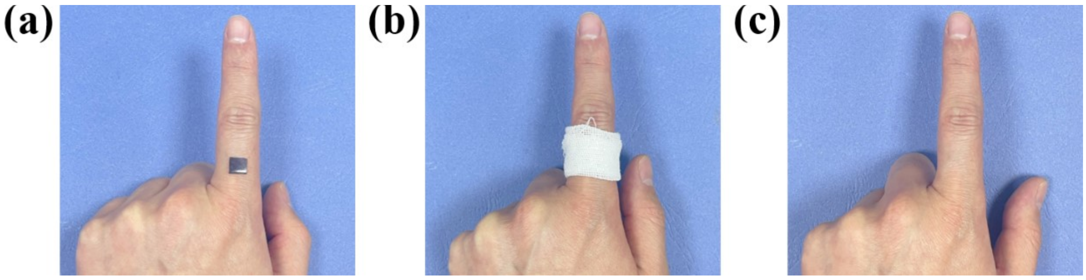

Fig. S15 (a) MPI-2 film attached to the finger, (b) 12 hours of skin adhesion, (c) skin condition after 12 hours.

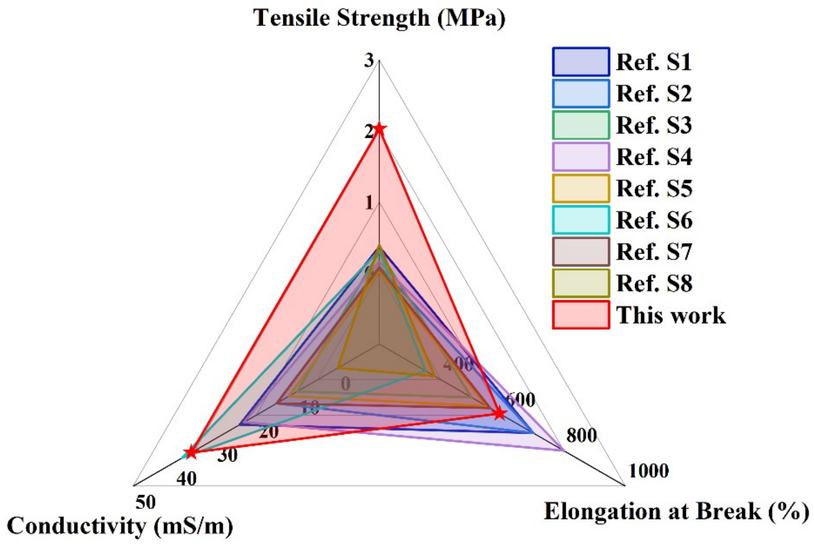

Fig. S16 Radar plots of tensile strength, conductivity and elongation at break of MPI-2 ionogel compared to other ionogels reported in the literature.[1-8]

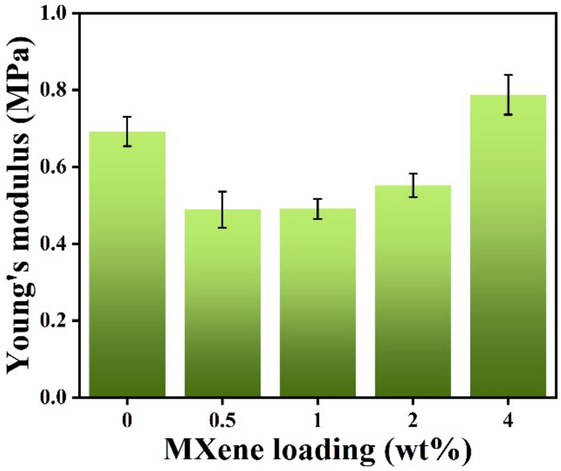

Fig. S17 Young's modulus of MPI ionogels with different MXene contents.

Reference

1. J. Sun, G. Lu, J. Zhou, Y. Yuan, X. Zhu and J. Nie, *ACS Appl. Mater. Interfaces*, 2020, **12**, 14272-14279.
2. B. Lei, L. Cao, X. Qu, Y. Liu, J. Shao, Q. Wang, S. Li, W. Wang and X. Dong, *Nano Research*, 2023, **16**, 5464-5472.
3. M. Zhang, X. Tao, R. Yu, Y. He, X. Li, X. Chen and W. Huang, *J. Mater. Chem. A*, 2022, **10**, 12005-12015.
4. J. Liu, X. Yang, M. Xu, H. Zhu, Y. Cheng, S. Li, T. Li, Y. Jiao and H. Song, *J. Mater. Chem. C*, 2023, **11**, 1184-1196.
5. M. Zammali, S. Liu and W. Yu, *Sens. Actuators, A*, 2021, **330**, 112855.
6. J. Tie, Z. Mao, L. Zhang, Y. Zhong, X. Sui and H. Xu, *Compos. B Eng.*, 2022, **232**, 109612.
7. A. Hu, C. Liu, Z. Cui, Z. Cong and J. Niu, *ACS Appl. Mater. Interfaces*, 2022, **14**, 12713-12721.
8. Q. He, Q. Zhong, Z. Sun, H. Zhang, Z. Zhao, Z. Shi, X. Liu, Z. Zhao, J. Lu, Y. Ye, Y. Wang, Y. Li, T. Xiang, J. Zhao and Y. Xie, *Nano Energy*, 2023, **113**, 108535.